

Energy dependence of transverse quark flow in heavy ion collisions

Péter Csizmadia¹ and Péter Lévai¹

¹ KFKI Research Institute for Particle and Nuclear Physics,
PO. Box 49, Budapest 1525, Hungary

Received 20 July 2004

Abstract. Energy dependence of quark transverse flow carries information about dynamical properties (equation of state, initial conditions) of deconfined matter produced in heavy ion collisions. We assume quark-antiquark matter formation in Pb+Pb collisions at CERN SPS and Au+Au collisions at RHIC energies and determine quark transverse flow at the critical temperature of the quark-hadron phase transition. Coalescence of massive quarks is calculated in the MICOR hadronization model and hadronic final state effects are considered using the GROMIT cascade program. Comparing theoretical results to data, transverse flow values are determined and energy dependence is discussed.

Keywords: transverse flow, hadronization, quark-antiquark matter, coalescence, recombination, final state interactions

PACS: 25.75.Nq

1. Introduction

In heavy ion collisions the formation of quark-gluon plasma (QGP) is expected at RHIC energies and above, however at lower energies we may not see a fully deconfined state. Although the precursors of the QGP state has been seen at CERN SPS [1], it is still controversial whether this new state of matter could really appear in this energy range. To retrieve information about the energy dependence of quark matter formation, experimental data must be compared to model calculations based on deconfinement in a wide energy range. Experimental data on transverse momentum spectra for different particle species existed at $\sqrt{s_{NN}} = 17.3 \text{ GeV}$ [2], 130 GeV [3, 4] and 200 GeV [5, 6]. Recently, NA49 Collaboration published new data at energies $\sqrt{s_{NN}} = 8.8 \text{ GeV}$ and 12.3 GeV ($E_{\text{lab}} = 40 A \text{ GeV}$ and $80 A \text{ GeV}$) [7, 8, 9, 10], which extended the accessible region.

In this paper we are interested in the transverse dynamics of heavy ion collisions. Transverse collective flow is directly related to the pressure of the central region with high energy density. Thus any jump (or discontinuity) in the flow can indicate modifications in the equation of state. We investigate hadronic transverse momentum spectra in the energy range $\sqrt{s_{\text{NN}}} = 8.8 - 200$ GeV and determine quark transverse flow before hadronization.

We assume the formation of deconfined matter with high energy density at all bombarding energies in the above mentioned energy range. Introducing critical temperature T_c for the quark-hadron phase transition, we assume a thermally equilibrated quark matter. The analysis of lattice-QCD results indicates the formation of a (constituent) quark-antiquark dominated deconfined matter at phase transition [11]. This quark-antiquark matter can be described by macroscopical parameters as temperature, particle densities and flow velocities. Here we consider T_c to be a uniform phase transition temperature at all collision energies. Quark densities and flow velocities are energy dependent. Since quark flow cannot be measured directly, we determine it indirectly from hadronic momentum spectra. We apply hadronization models based on coalescence of massive quarks and antiquarks with small relative momentum (ALCOR model [12, 13] to reproduce particle yields and MICOR [14, 15] to reproduce transverse momentum spectra at low momenta, $p_T < 2$ GeV). Our analysis is based on the MICOR model implementing different quark flow velocities and calculated results are compared to measured data. In parallel we will investigate the influence of hadronic rescattering on hadronic flow by the GROMIT cascade program [16].

Recently parton coalescence models were applied successfully at RHIC energies in the intermediate momentum region ($2 < p_T < 6$ GeV) to explain the measured anomalous p^+/π^+ and \bar{p}^-/π^- ratios and reproduce the measured transverse momentum spectra [17, 18, 19]. In parallel, application of parton coalescence can reproduce the measured properties of the elliptic flow at RHIC energies [19, 20, 21]. The success of these calculations supports the application of quark coalescence in a wide momentum region. The MICOR model offers the possibility to investigate coalescence, especially flow phenomena, in low- p_T region.

2. Calculations with the MICOR model

In our model the expanding quark-antiquark matter cools down to critical temperature, $T_c = 170$ MeV, where hadronization starts. The longitudinally expanding deconfined matter is limited to the coordinate rapidity region $\eta = [-\eta_{\text{max}}, +\eta_{\text{max}}]$. Inside this region we assume constant (anti)quark densities, $dN_{\bar{u}}/d\eta$. We use the following notation for the numbers of newly produced quark-antiquark pairs at T_c :

$$N_{u\bar{u}} = N_{d\bar{d}} = N_{q\bar{q}}/2, \quad N_{s\bar{s}} = f_s N_{q\bar{q}}. \quad (1)$$

In the MICOR model final hadron numbers are scaled linearly on the initial quark numbers. This linear scaling remains valid for the rapidity densities also.

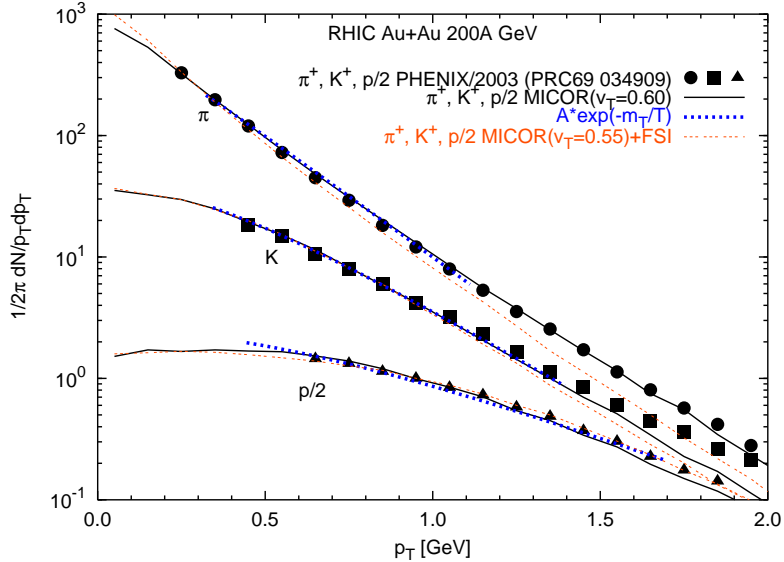


Fig. 1. Transverse momentum spectra for π^+ , K^+ , and p at $\sqrt{s_{NN}} = 200$ GeV in AuAu collisions (dots, squares and triangulaires) [5]. Full lines indicate quark coalescence results at $v_T = 0.60$, neglecting final state interactions. Thick dashed lines show the applied exponential fits to extract slope parameters. Thin dotted lines indicate the MICOR results at a smaller transverse flow, $v_T = 0.55$, but including final state interactions (FSI).

In the ALCOR calculations for mid-rapidity data one can see the collision energy dependence of the number of newly produced quark-antiquark numbers [13], which can be described approximately as $dN_{q\bar{q}}/dy = 130 \cdot \ln(\sqrt{s_{NN}}/2.5)$ [23].

The MICOR model covers wide space-time rapidity region and it reproduces measured mid-rapidity momentum spectra by the following parameters: $\eta_{\max} = 1.9$, $N_{q\bar{q}} = 720$, $f_s = 0.35$ at $\sqrt{s_{NN}} = 17.3$ GeV (SPS), and $\eta_{\max} = 4$, $N_{q\bar{q}} = 3800$, $f_s = 0.26$ at $\sqrt{s_{NN}} = 200$ GeV (RHIC). At different SPS energies the above $N_{q\bar{q}}$ value is scaled by the measured charged particle yield, as well as at RHIC energies. (A detailed analysis will be published elsewhere [24].)

The inverse slopes for transverse hadronic momentum spectra depend on the quark flow but not on the quark number. Secondary interactions among hadrons depend on absolute hadron numbers. We can set all above mentioned parameters of MICOR, but left only one parameter free, namely the quark transverse flow, v_T . We investigate the v_T dependence of hadronic transverse momentum spectra of different hadronic species. In this comparison, as one of the possibilities, we will assume fast hadronization and neglect final state interactions.

We consider π^+ , K^+ , and p transverse momentum spectra at $\sqrt{s_{NN}} = 200$ GeV [5] in AuAu collisions, see Figure 1. We expect an energetic collision with a fast expansion and fast hadronization. In this case we can compare the MICOR results

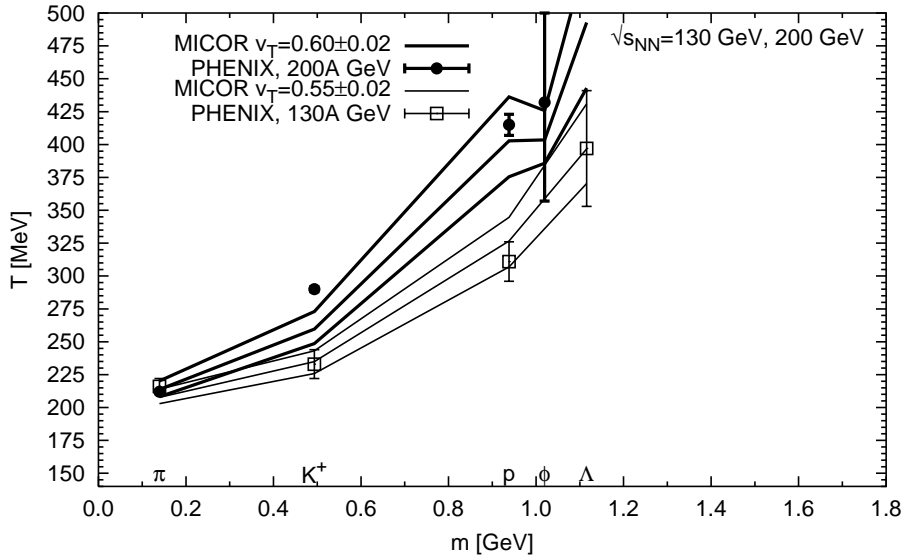


Fig. 2. Inverse slopes from MICOR model and RHIC experiment. MICOR points are connected by thin lines for $v_T = 0.55 \pm 0.02$ flow velocities and thick lines for $v_T = 0.60 \pm 0.02$. $\sqrt{s_{NN}} = 130$ GeV data points from PHENIX [3] are denoted by open squares, 200 GeV points from PHENIX [5] are denoted by dots.

(full lines) to the experimental data directly. The agreement between MICOR ($v_t = 0.6$) and the data points at $0.2 < p_T < 1.5$ GeV indicates the validity of the above expectation. Dashed lines show exponential fits to the calculated spectra.

On the other hand, we are able to switch on hadronic interactions in the final state by using the GROMIT transport code [16]. However, GROMIT needs space-time information, which was integrated out in the MICOR model. Here a cylindrical symmetric matter was assumed with uniform densities, longitudinal Bjorken flow and constant transverse flow.

The number of secondary collisions suffered by a particle moving with velocity v can be determined using the following rough estimate:

$$N_{\text{coll}}(v) \sim \int_{t_0}^{\infty} n(t) \sigma v dt \sim \int_{t_0}^{\infty} \frac{C'}{t^{\alpha} \bar{v}_{\text{flow}}} \sigma v dt = \frac{C \sigma v}{\bar{v}_{\text{flow}}} , \quad (2)$$

where $n(t)$ is the density of the matter at the location of the particle at time t and σ denotes the averaged cross section. The density, $n(t)$, is supposed to be inversely proportional to the average flow velocity \bar{v}_{flow} and a power of the elapsed time t^{α} . If the exponent α is a constant, then C is also constant. The average flow velocity in our case can be approximated by the transverse quark flow velocity v_T . The result of this simple calculation is that a particle suffers at least one collision ($N_{\text{coll}}(v) \geq 1$)

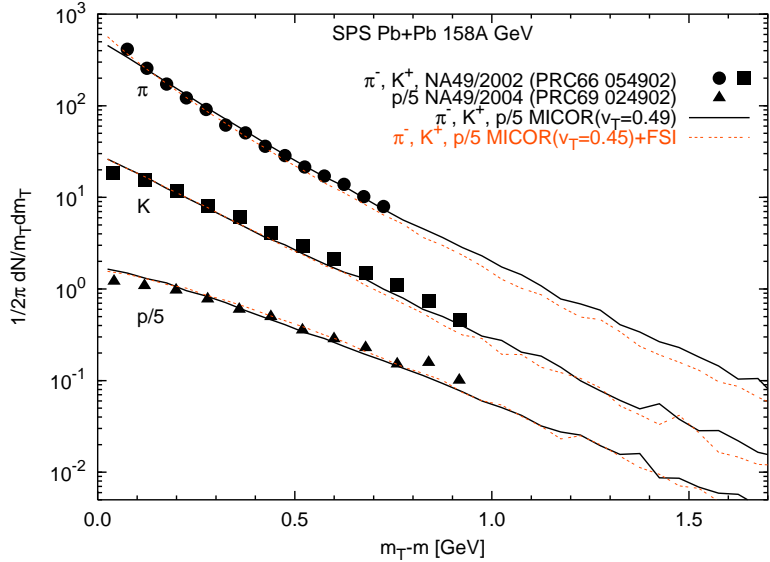


Fig. 3. Transverse momentum spectra for π^+ , K^+ , and p at $\sqrt{s_{NN}} = 17.3$ GeV in PbPb collisions (dots, squares and triangulairs) [7, 8]. Full lines indicate quark coalescence results at $v_T = 0.60$, neglecting final state interactions.

if its individual velocity v satisfies the following relation:

$$v \geq v_T^{\text{flow}} / C\sigma. \quad (3)$$

Now switching on final state interactions (thin dotted lines) and focusing on proton spectra, we are able to reproduce proton data with a smaller quark flow superposed with the gained transverse energy during secondary interactions. On the other hand, the calculated light meson spectra will deviate from data, because the “pion wind” decreases the pion yield at higher momenta. From Figure 1 we can claim that there is no free room for final state interactions. Assuming fast hadronization, we are able to reproduce experimental data. However, if we want to include light mesons produced via independent jet-fragmentation, then the second case with final state interaction looks more favourable, where extra meson yields can be accommodated. (Contribution from jet fragmentation appears at much higher p_T for protons.) At this point we can not decide between the two investigated scenarios. Further analysis of perturbative QCD contributions is needed, similarly to Refs. [17, 18, 19] and Ref. [22].

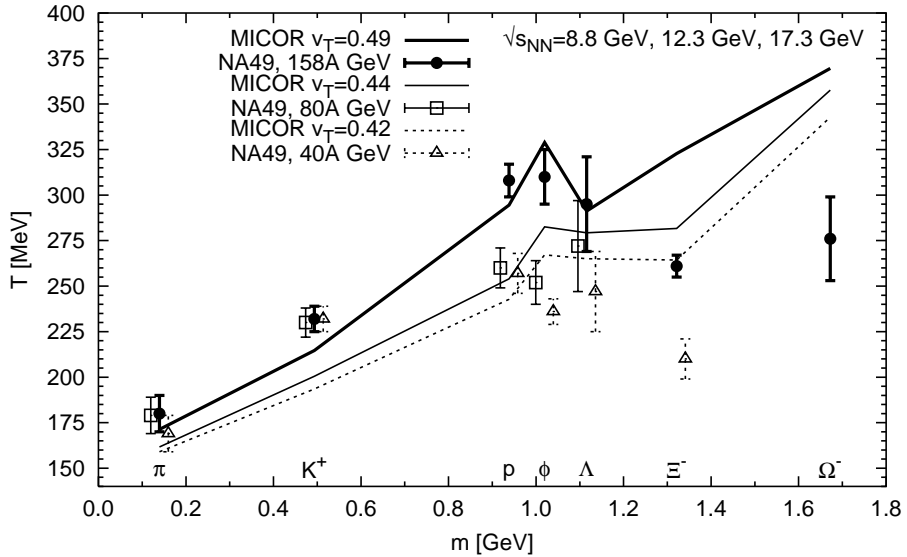


Fig. 4. Inverse slopes from MICOR model without final state interactions and experimental data from NA49 [7, 8, 9, 10]. MICOR points are connected by dotted lines for $v_T = 0.42$ flow velocity, thin lines for $v_T = 0.44$ and thick lines for $v_T = 0.49$. Experimental data points at 40 A GeV are denoted by open triangles, 80 A GeV data are displayed by squares, 158 A GeV data are indicated by filled dots.

Figure 2 summarizes our results on slope parameters obtained in MICOR, when final state interactions are neglected. The uncertainties in quark transverse flow are displayed selecting $v_T = 0.55 \pm 0.02$ at $\sqrt{s_{NN}} = 130$ GeV (thin lines) and $v_T = 0.60 \pm 0.02$ at $\sqrt{s_{NN}} = 200$ GeV (thick lines). The MICOR results agree with the measured slopes quite well, which agreement confirms the application of MICOR model and the assumption of quark-antiquark matter formation at RHIC.

At SPS we expect slower expansion and hadronization, which yield to a less energetic collision dynamics. Thus after hadronization, secondary interactions may have a larger role to reshape the final momentum distributions and modify the inverse slopes. To validate this expectation, we repeat our MICOR calculation at SPS energies with and without final state interactions.

Figure 3 displays the MICOR result for π^+ , K^+ , and p transverse momentum spectra at $\sqrt{s_{NN}} = 17.3$ GeV [7, 8] in PbPb collisions at SPS. Without final state interactions (full lines) one can reproduce the pion and proton data at $v_T = 0.49$. For kaons we find slight deviation. Introducing final state interactions and focusing on the proton spectra, we obtain $v_T = 0.45$. Proton spectra is reproduced in both cases. Kaon and pion spectra are similar where data are available. However, final state interactions modify pion and kaon spectra by decreasing the yield at higher p_T . The obtained suppression in the spectra at SPS is much less than at RHIC.

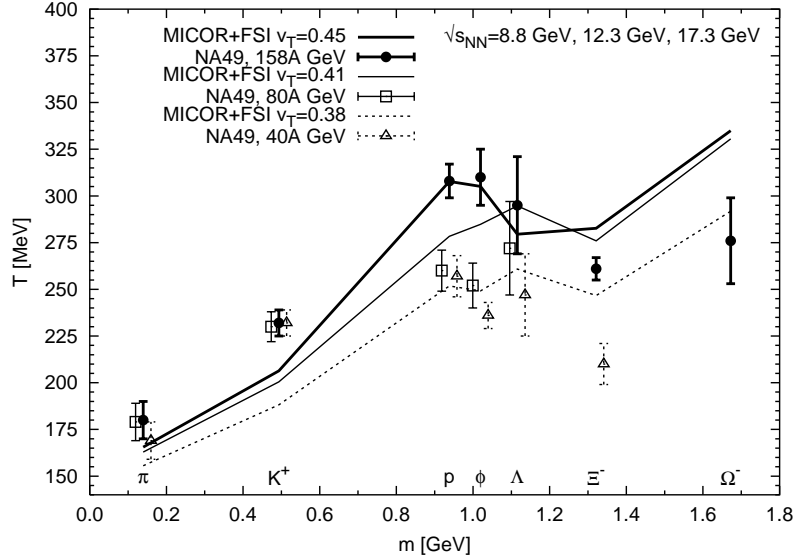


Fig. 5. Inverse slopes from the MICOR model including final state interactions on NA49 experimental data [7, 8, 9, 10]. MICOR points are connected by dotted lines for $v_T = 0.38$ flow velocity, thin lines for $v_T = 0.40$ and thick lines for $v_T = 0.44$. 40 A GeV experimental data points are denoted by open triangles, 80 A GeV points are open squares, 158 A GeV points are filled circles.

The displayed differences between data and the MICOR calculation with final state interaction indicate that hadronic collisions can become important in a wide energy range. However, we need to investigate whether pQCD processes (namely independent jet fragmentation) could provide the missing contributions both at RHIC and SPS energies.

Now we summarize MICOR results on transverse slopes at projectile energies $E_{beam} = 40, 80, 158$ AGeV at SPS. Figure 4 shows the slopes in case of neglecting final state interactions. Figure 5 displays the slopes for including final state effects. In the latter case experimental data can be reproduced by transverse flow $v_T^{(FSI)} = 0.38, 0.40, 0.44$, respectively. These v_T values are smaller than in the interactionless case, the difference is $v_T^{(noFSI)} - v_T^{(FSI)} \simeq 0.04$. It means that final state interactions increase transverse flow effect. Thus we can start from smaller quark flow values for the expanding quark matter, after switching on hadronic interactions the hadronic transverse momentum spectra will be reproduced.

Inverse slopes on Figure 5 are fitted at low p_T ($p_T < 1$ GeV). There is a small difference between data and calculations at smaller collision energies, even for the best choice of the v_T values. Pion and kaon inverse slopes from MICOR are significantly higher than data at $E_{beam} = 40, 80$ AGeV. At larger energy, $E_{beam} = 158$ AGeV, the agreement is recovered using $v_T = 0.44 \pm 0.02$.

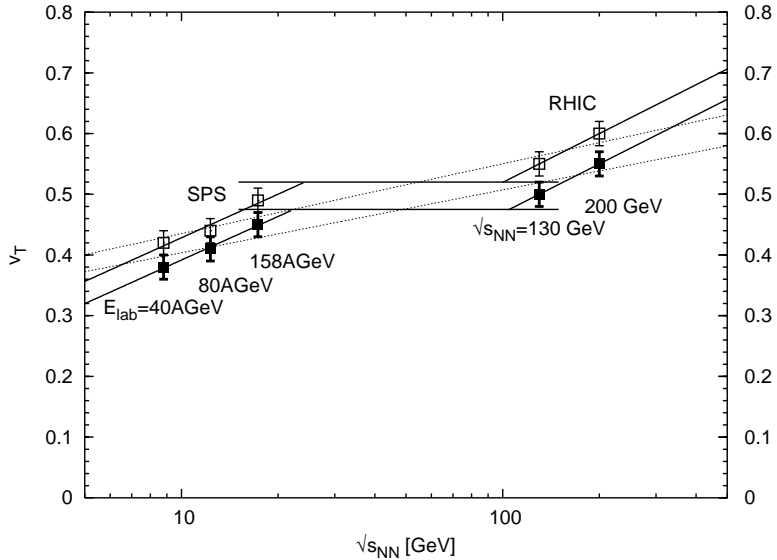


Fig. 6. The energy dependence of the average transverse flow velocities of the expanding quark matter in the MICOR model including final state effects (full boxes) and neglecting them (open boxes).

Now the results of Figures 2, 4 and 5 can be combined into one figure to display energy dependence of transverse quark flow, $v_T(\sqrt{s_{NN}})$, see Figure 6. Including final state interactions (full boxes) we obtain smaller values for the quark flow than neglecting them in a fast hadronization scenario (open boxes). The uncertainties on the transverse flow values allow us to construct two interpretations.

First we can assume a simple logarithmic energy dependence (dotted lines). If we neglect final state effects, then we can draw the following line to guide the eyes

$$v_T(\sqrt{s_{NN}}) = 0.32 + 0.050 \cdot \ln(\sqrt{s_{NN}}) . \quad (4)$$

Including final state effects the energy dependence of the quark transverse flow is

$$v_T(\sqrt{s_{NN}}) = 0.30 + 0.045 \cdot \ln(\sqrt{s_{NN}}) . \quad (5)$$

Here the energy $\sqrt{s_{NN}}$ is measured in GeV.

On the other hand, our results obtained in discrete energy points may give a hint for a plateau between the largest CERN SPS and the smallest accessible RHIC energies (solid lines). Further studies are needed to decide if this hypothetical plateau exists at all and what are the theoretical consequences. The existence of such a plateau could yield important information about the equation of state of deconfined matter.

The increasing transverse quark flow can not violate causality, thus it will saturate. However, this saturation seems to appear well beyond RHIC energies.

3. Conclusions

In this paper we summarized our results on the energy dependence of quark transverse flow. We assumed that deconfined matter was produced at SPS and RHIC energies in central Pb+Pb and Au+Au collisions and an initial quark transverse flow has been developed before hadronization. Using the MICOR hadronization model we could extract quark transverse flow parameters at phase transition. The comparison of calculated hadronic transverse momentum spectra and measured ones yields quark flow values with high precision in a wide energy region. Assuming fast hadronization and neglecting final state hadronic collisions, one can determine the wanted energy dependence for quark flow. We are pleased to see the good agreement between data and our quark based hadronization model calculations at low- p_T ($p_T < 1$ GeV).

Using the GROMIT transport code, one can investigate the influence of final state hadronic effects. In this case smaller quark flow values can be used to reproduce experimental data. At first we reproduce the proton transverse momentum spectra. Applying the extracted quark flow, the pion and kaon spectra will be smaller than the experimental ones. However, this deviation allows us to include meson production from independent jet fragmentation, determined by perturbative QCD calculations. These perturbative contributions become comparable to the quark coalescence yield in the region $p_T \geq 1$ GeV for pions and kaons. A detailed perturbative QCD calculation is needed to determine the interplay between perturbative, quark coalescence and hadronic contributions for light mesons. For heavy baryons and antibaryons the perturbative contributions are negligible in the region $p_T \leq 4$ GeV, where coalescence and secondary hadronic interactions dominate their momentum spectra.

The energy dependence of the obtained quark transverse flow values can be described by a simple logarithmic increase. On the other hand, the high precision of the extracted flow values may indicate the possible existence of a plateau between SPS and available RHIC energies. Further analysis of the existing experimental data is needed to confirm this plateau. In parallel, new data would be needed in the energy range $20 \leq \sqrt{s_{NN}} \leq 130$ GeV to determine the energy dependence more precisely.

Acknowledgments

The authors are grateful to Gyuri Wolf for organizing the Budapest'04 Workshop and for providing an excellent scientific and social atmosphere. We thank Brian A. Cole for his comments. This work was supported by Hungarian OTKA grant T043455, T038406.

References

1. CERN Press Release of Feb. 10, 2000; U. Heinz, M. Jacob, [nucl-th/0002042](#).
2. P.G. Jones et al. (NA49 Coll.), *Nucl. Phys.* **A610** (1996) 188c-199c; C. Bormann et al. (NA49 Coll.), *J. Phys.* **G23** (1997) 1817-1825.
3. K. Adcox et al. (PHENIX Coll.), *Phys. Rev. Lett.* **89** (2002) 092302; *Phys. Rev.* **C69** (2004) 024904.
4. J. Adams et al. (STAR Coll.), *Phys. Rev. Lett.* **89** (2002) 092301; [nucl-ex/0206008](#); [nucl-ex/0306029](#); [nucl-ex/0311017](#); *Phys. Rev. Lett.* **92** (2004) 182301.
5. S.S. Adler et al. (PHENIX Coll.), *Phys. Rev. Lett.* **91** (2003) 072301; *Phys. Rev.* **C69** (2004) 034909.
6. J. Adams et al. (STAR Coll.), *Phys. Rev. Lett.* **92** (2004) 112301; [nucl-ex/0406003](#).
7. S.V. Afanasiev et al. (NA49 Coll.), *Phys. Rev.* **C66** (2002) 054902.
8. T. Anticic et al. (NA49 Coll.), *Phys. Rev.* **C69** (2004) 024902.
9. C. Alt et al. (NA49 Coll.), *J. Phys.* **G30** (2004) S119-S128.
10. T. Anticic et al. (NA49 Coll.), *Phys. Rev. Lett.* **93** (2004) 022302.
11. P. Lévai, U. Heinz, *Phys. Rev.* **C57** (1998) 1879.
12. T.S. Biró, P. Lévai and J. Zimányi, *Phys. Lett.* **B347** (1995) 6.
13. T.S. Biró, P. Lévai and J. Zimányi, *J. Phys.* **G27** (2001) 439; *J. Phys.* **G28** (2002) 1561.
14. P. Csizmadia, P. Lévai, S.E. Vance, T.S. Biró, M. Gyulassy, J. Zimányi, *J. Phys.* **G25** (1999) 321; P. Csizmadia and P. Lévai, *Phys. Rev.* **C61** (2000) 031903; P. Lévai, T.S. Biró, P. Csizmadia, T. Csörgő, J. Zimányi, *J. Phys.* **G27** (2001) 703.
15. P. Csizmadia and P. Lévai, *J. Phys.* **G28** (2002) 1997.
16. S. Cheng, S. Pratt, P. Csizmadia, Y. Nara, D. Molnár, M. Gyulassy, S.E. Vance, B. Zhang, *Phys. Rev.* **C65** (2002) 024901.
17. R.C. Hwa, C.B. Yang, *Phys. Rev.* **C66** (2002) 025205; *Phys. Rev. Lett.* **90** (2003) 212301; [nucl-th/0401001](#).
18. R.J. Fries, B. Müller, C. Nonaka, S.A. Bass, *Phys. Rev. Lett.* **90** (2003) 202303. *Phys. Rev.* **C68** (2003) 044902.
19. V. Greco, C.M. Ko, P. Lévai, *Phys. Rev. Lett.* **90** (2003) 202302; *Phys. Rev.* **C68** (2003) 034904.
20. D. Molnár, S.A. Voloshin, *Phys. Rev. Lett.* **91** (2003) 092301; Z. Lin, D. Molnár, *Phys. Rev.* **C68** (2003) 044901.
21. P.F. Kolb, L.W. Chen, V. Greco, C.M. Ko, *Phys. Rev.* **C69** (2004) 051901.
22. Y. Zhang, G. Fai, G. Papp, G.G Barnaföldi, and P. Lévai, *Phys. Rev.* **C65** (2002) 034903.
23. P. Lévai, J. Zimányi, T.S. Biró, in preparation.
24. P. Csizmadia, P. Lévai, in preparation.